



ELSEVIER

Journal of Crystal Growth 241 (2002) 108–114

JOURNAL OF
**CRYSTAL
GROWTH**

www.elsevier.com/locate/jcrysgr

Growth, characterization and nonlinear optical properties of SrB_4O_7 crystals

Feng Pan*, Guangqiu Shen, Ruji Wang, Xiaoqing Wang, Dezhong Shen

Department of Chemistry, Tsinghua University, Beijing 100084, People's Republic of China

Received 24 May 2001; accepted 16 January 2002

Communicated by R.S. Feigelson

Abstract

High optical quality crystals of strontium tetraborate SrB_4O_7 (SBO) have been grown by the Kyropoulos method. The structure of SBO has also been determined. The FWHM of the X-ray rocking curve on the (0 2 1) plane was 0.005° . The optical and nonlinear optical properties of the SBO crystal were investigated. The absorption edge in the vacuum UV spectra of the SBO was below 120 nm. Some SHG effects were also investigated. © 2002 Elsevier Science B.V. All rights reserved.

PACS: 42.70.Mp; 81.10.-h; 78.20.Ci

Keywords: A1. Crystal structure; A2. Kyropoulos method; B1. Borates; B1. Strontium compounds; B2. Nonlinear optical materials

1. Introduction

A series of borates, such as barium borate $\beta\text{-BaB}_2\text{O}_4$ (BBO) and lithium triborate LiB_3O_5 (LBO), are well-known nonlinear optical crystals. They are widely used for harmonic generation of laser radiation to produce new laser sources in the visible and UV spectral ranges [1]. In recent years, more promising borate materials have been discovered and studied, including cesium triborate CsB_3O_5 [2], cesium lithium borate $\text{CsLiB}_6\text{O}_{10}$ (CLBO) [3], lithium diborate $\text{Li}_2\text{B}_4\text{O}_7$ [4], $\text{KBe}_2\text{BO}_3\text{F}$ (KBBF) [5], $\text{Sr}_2\text{Be}_2\text{B}_2\text{O}_7$ (SBBO) [6], etc.

One of the main aims of this research area is to find novel NLO crystal materials with UV cutoffs that are as short as possible.

Strontium tetraborate SrB_4O_7 (SBO) has been investigated as a potential NLO material with some excellent mechanical and optical properties such as high powder SHG coefficient, high optical damage threshold, high hardness, etc. [7,8]. The most important reason for our further investigation on growing SBO crystals is their high UV transmittance at wavelengths down to about 130 nm. The current results also indicate some errors or shortcomings in the previous results.

Large SrB_4O_7 single crystals with high optical qualities were grown using the Kyropoulos method. Their structure was determined and the refractive indices were measured in the visible

*Corresponding author. Tel.: +86-10-6277-2109; fax: +86-10-6277-1149.

E-mail address: ppfeng@263.net (F. Pan).

region especially at some important wavelengths not reported in the previous publications. The optical transparency was measured from the vacuum UV to IR regions. The nonlinear optical behavior of the SBO crystal is also discussed.

2. Crystal growth and structure

SrB_4O_7 crystals were grown from a stoichiometric melt of SrCO_3 (>99.5%) and H_3BO_3 (>99.9%). Both powders were ground together and then put into a platinum crucible 64 mm in diameter and 50 mm in height. According to the phase equilibrium diagram for the $\text{SrO}-\text{B}_2\text{O}_3$ system [9], SrB_4O_7 congruently melts at $994 \pm 10^\circ\text{C}$. Therefore, the mixture was placed in a furnace and heated to 1030°C for melting. The crucible was rotated several times in one direction and then several times in the other direction at 30 rpm for 12–16 h to homogenize the melt. Seed crystals were obtained by spontaneous crystallization. A small crystal oriented along the c -axis was attached as a seed to a platinum rod and came in contact with the melt surface at a temperature of $986\text{--}987^\circ\text{C}$. With the appropriate temperature gradient control with the vertical gradient shown in Fig. 1, while maintaining the oscillating crucible rotation, the melt temperature was reduced to

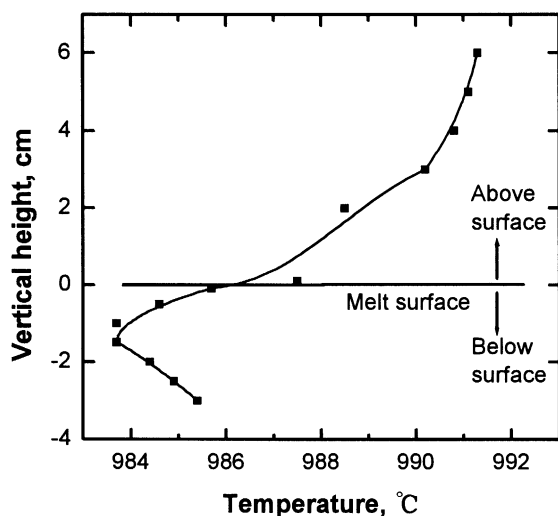


Fig. 1. Vertical temperature gradient in SBO growth procedure.

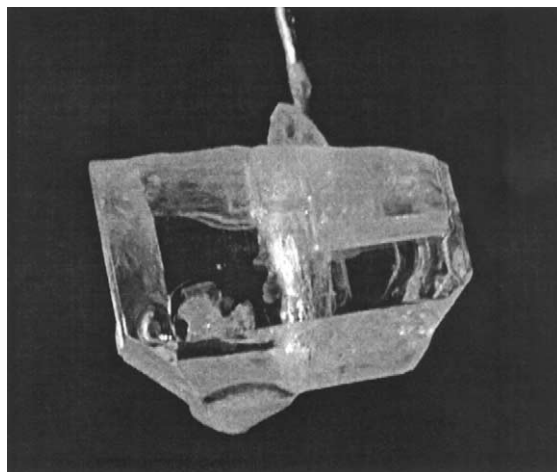


Fig. 2. SBO crystal with a size of $35 \times 25 \times 25 \text{ mm}^3$ grown using Kyropoulos method. The opaque crystal exists in the surface of the bulk only.

985°C at a rate of $0.25^\circ\text{C}/\text{day}$ until the end of the growth process. After 6 days, a transparent, colorless SBO single crystal was obtained with an approximate size of $35 \times 25 \times 25 \text{ mm}^3$, as shown in Fig. 2. This crystal had well-developed facets that match the sketch shown in Ref. [7]. The facets are limited by the growth method and temperature gradient. In these experiments, the seed just came in contact with the melt surface, so the shape of the crystal does not follow the isotherm.

Generally, borate melts are quite viscous, so the relatively fast oscillating crucible rotation is necessary during crystal growth for more complete homogenization and more effective mass transportation. The extremely slow cooling rate used here helped to reduce the crystal defects resulting from the slow mass transportation in the viscous system.

The rocking curve of the (021) plane was measured to examine the SBO crystal quality. The theta-scale was scanned from 20.600° to 20.900° with a step of 0.002° . The FWHM is very small, $\Delta\theta_{021} = 0.005^\circ$, which indicates that the crystal lattice is nearly perfect and the SBO crystal quality is quite high.

A single crystal of dimensions $0.1 \times 0.4 \times 0.4 \text{ mm}^3$ was selected for structural determination on a Brüker P4 diffractometer. The data

collection and processing parameters are listed in Table 1.

The SBO crystal structure was reported by Perloff and Block [10] and Krogh-Moe [11] in 1960s. To facilitate the comparison of their results with this work, the data listed in Table 2 have been converted to the same origin and space-group orientation (Pmn2₁).

The *x* and *y* parameters reported by the previous authors agreed well with each other; however, the *z* parameters were very different. Perloff and Block [10] indicated that the false mirror planes at *z* = 0 and 0.5 in the electron-density map derived from the phases based only on the Sr contribution led to Krogh-Moe's misplaced

O(2) and B(1). Their refinements using their model with Krogh-Moe's observed data and Krogh-Moe's model with their observed data confirmed their observation [10]. However, Perloff and Block's structure is a different enantiomorph from our structure. Refinement using Perloff and Block's parameters for our 1667 observed data which converged to *R* = 0.0998 (as opposed to our value of 0.0507) suggests that our structure as described below is the correct one.

The structure consists of a three-dimensional borate network with channels parallel to the *a*- and *b*-axis with Sr ions located in these channels (see Figs. 3 and 4). All the boron atoms are tetrahedrally coordinated and all the tetrahedra are

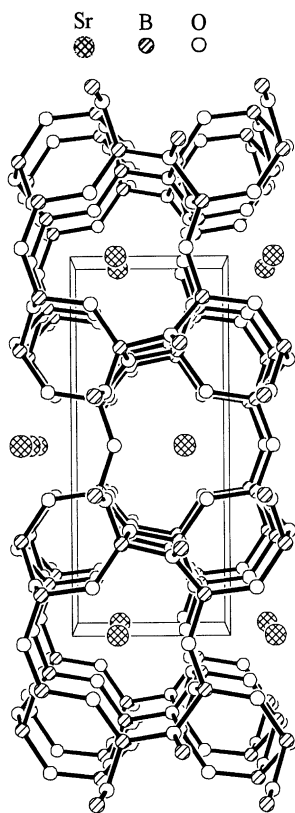
Table 1
Data collection and processing parameters

Molecular formula	SrB ₄ O ₇
Molecular weight	242.86
Color and habit	Colorless plate
Crystal size	0.1 × 0.4 × 0.4 mm ³
Crystal system	Orthorhombic
Space group	P2 ₁ nm (No. 31)
Unit cell parameters	<i>a</i> = 4.2392(11) <i>α</i> = 90.00 <i>b</i> = 4.447(3) <i>β</i> = 90.00 <i>c</i> = 10.724(2) <i>γ</i> = 90.00 <i>V</i> = 202.14(14) <i>Z</i> = 2 <i>F</i> (0 0 0) = 228
Density (calculated)	3.990 g/cm ³
Diffractometer	Brüker P4
Radiation	Graphite-monochromatized Mo K _α , λ = 0.71073 Å
Temperature	295 ± 2 K
Scan type	ω-scan
Data collection range	−8 < <i>h</i> < 8, −8 < <i>k</i> < 8, −21 < <i>l</i> < 21; θ _{max} = 45°
Reflections measured	Total: 1874; Unique (<i>n</i>): 1722; Observed [<i>I</i> ≥ 2σ(<i>I</i>): 1667
Absorption coefficient	13.312 mm ^{−1}
Min and max transmission	0.19681, 0.29359
Background counting	Stationary counts for one-fourth of scan time at each end of scan range
No. of variables, <i>p</i>	59
	$w = \frac{1}{\sigma^2(F_o^2) + (0.0898P)^2 + 0.8000P}$
	$P = (F_o^2 + 2F_c^2)/3$
R1 (for all reflections)	0.0519
wR2 (for all reflections)	0.12040
S	1.002
Largest and mean Δ/σ	0.000, 0.000
Residual extrema in final difference map	−6.773–3.052 e Å ^{−3}

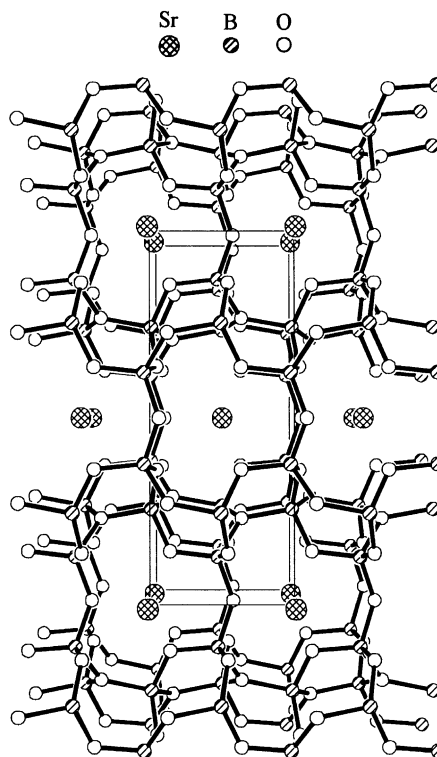
Table 2

Comparison of previous and present results, converted to the same origin and space group orientation ($Pmn2_1$)

Atoms	From Perloff and Block's paper			From Krogh-Moe's paper			This paper		
	<i>x</i>	<i>y</i>	<i>z</i>	<i>x</i>	<i>y</i>	<i>z</i>	<i>x</i>	<i>Y</i>	<i>z</i>
Sr	0	0.288	0	0	0.289	0	0	0.228	0
O(1)	0	0.728	0.415	0	0.728	0.454	0	0.726	0.576
O(2)	0.359	0.858	0.953	0.359	0.857	0.064	0.359	0.856	0.041
O(3)	0.365	0.225	0.356	0.365	0.226	0.335	0.365	0.226	0.632
O(4)	0.223	0.632	0.353	0.221	0.631	0.335	0.223	0.632	0.636
B(1)	0.378	0.173	0.041	0.379	0.174	0.976	0.378	0.174	0.969
B(2)	0.248	0.677	0.006	0.246	0.671	0.963	0.249	0.679	0.995

Fig. 3. Polyhedral representation of strontium tetraborate along the *a* direction.

connected to each other by sharing corners (Fig. 5). Four independent O atoms can be divided into two groups: O(1), O(2) and O(3) are linked to two B atoms with shorter O–B bonds (1.416–1.458 Å), while O(4) is linked to three B atoms with longer O–B bonds (1.536–1.560 Å). The Sr atom is

Fig. 4. Polyhedral representation of strontium tetraborate along the *b* direction.

surrounded by 9 oxygen atoms to form a capped cube-coordination environment (see Fig. 6).

Although there are six-membered B–O rings in the borate network parallel to the *b*-axis, the rings do not belong to the “conjugated group” type, which is considered to be an important cause of

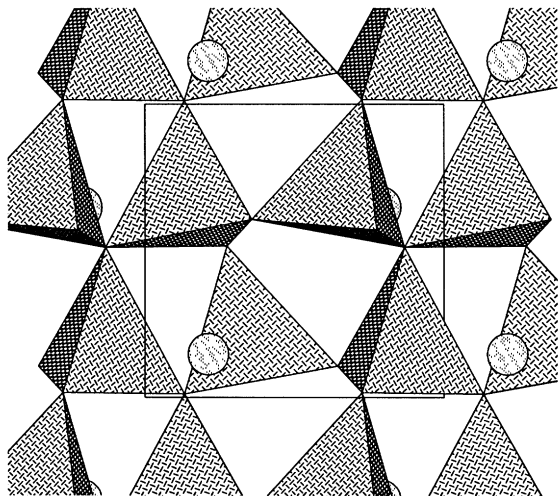


Fig. 5. Polyhedral representation of strontium tetraborate along the c direction.

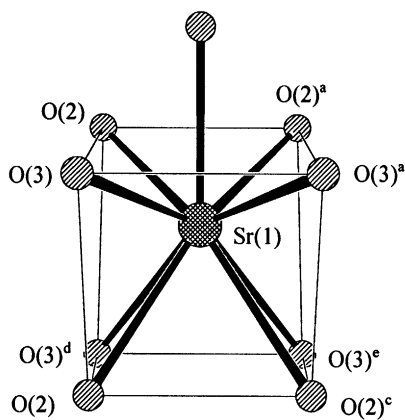


Fig. 6. Coordination polyhedron of strontium atom (capped cube).

large SHG coefficient according to the “theory of anionic groups” [12]. An analysis of the relationship between this “exceptional” op. cit. structure and its remarkable microscopic optical nonlinear effect will be published in another paper.

SBO crystals were not found to be hygroscopic.

3. Optical properties

The refractive indices of the SBO crystal were measured using two prisms with an angle of about

$28^{\circ}30'$. Both prisms were oriented. The measured results are listed in Table 3. The values of the refractive indices in the IR spectra were extrapolated according to the Sellmeier equation

$$n^2(\omega) = n_0 + A/(\omega^2 - B) + C\omega^2 \quad \text{for } n_x, n_y,$$

$$n^2(\omega) = n_0 + A/(\omega^2 - B) + C/(\omega^2 - D) \quad \text{for } n_z.$$

The coefficients n_0 , A , B , C and D are listed in Table 4.

The main optical axes are marked as $X-b$, $Y-a$, $Z-c$ where a , b and c are the crystallographic axes so that $n_x < n_y < n_z$. The differences between n_x , n_y and n_z are not as small as that reported in Ref. [7]. Some values were measured at key wavelengths such as 5320 Å. However, our calculation confirmed the conclusion of Oseledchik et al. [7], that the birefringence of SBO is very small for phase matching for SHG or sum-frequency generation.

An a -oriented SBO single crystal with a size of $10 \times 8 \times 2 \text{ mm}^3$ was polished on both sides for transparency measurements in a vacuum UV spectrometer and an infrared spectrometer. The transparency of the SBO sample was measured from 120–4000 nm with the results shown in Fig. 7.

Our results differ in some aspects from the data of Oseledchik et al. [7]. Our spectra showed two absorption peaks at wavelengths of about 150–214 nm in the vacuum UV region, which should be investigated further. In contrast to the results of

Table 3
Refractive indices of SBO crystal

Wavelength λ (Å)	n_x	n_y	n_z
4047	1.7487	1.7510	1.7530
4358	1.7447	1.7469	1.7489
4860	1.7399	1.7419	1.7440
5145	1.7378	1.7397	1.7419
5320	1.7366	1.7385	1.7407
5461	1.7358	1.7376	1.7398
5790	1.7340	1.7358	1.7380
5893	1.7335	1.7353	1.7375
6561	1.7306	1.7324	1.7346
6943	1.7292	1.7310	1.7330
8000	1.7257	1.7278	1.7277
10000	1.7202	1.7229	1.7370
10140	1.7198	1.7226	1.7362
10640	1.7184	1.7215	1.7344

Table 4

Coefficients of Sellmeier's equation for SBO

	n_0	A	B	C	D
n_x	2.98275	1.09951×10^6	2.81466×10^6	-3.49519×10^{-10}	—
n_y	2.98113	1.28301×10^6	1.98803×10^6	-2.56313×10^{-10}	—
n_z	2.98462	360811.0	8.04077×10^7	1.41513×10^6	1.32839×10^6

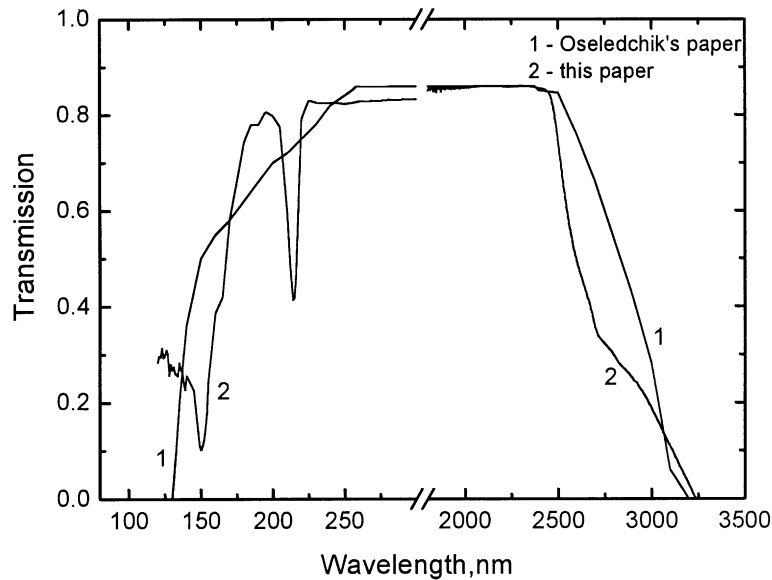


Fig. 7. Transparency of the SBO crystal.

Oseledchik et al. [7], we found SBO to be transparent to below 120 nm, making it unique among NLO crystals.

4. Nonlinear optical properties

Although the optical nonlinearity of SBO powder was found to be approximately the same as that of KTP [7], its optical birefringence was quite small for phase matching for SHG of 1.064 micron. However, SHG of Nd:YAG laser radiation ($\lambda = 1064$ nm) was observed on an oriented and polished SBO crystal with dimensions $9 \times 7 \times 6$ mm³. The maximum green output appeared when the incident beam transmitted along the b -axis and the angle between polarization

plane of laser beam and the a - or c -axis was about 45° . It was estimated that the conversion efficiency for SHG was $< 1\%$. The mechanism needs further study, but may not be attributed to noncoherent SHG in the surface layer of the SBO crystal, because the output intensity varied in different directions.

No linear electro-optical effect was detected in these SBO crystals.

5. Conclusion

Large SBO single crystals were successfully grown using the Kyropoulos method. Several physical and optical properties were investigated to update the refractive indices and to provide

detailed transparency measurements, especially in the vacuum UV region. It was discovered that the transparency increases rapidly at 150 nm and does not cut off until 120 nm, which is a very important consideration for the vacuum UV spectral lasers. However, its use in this application is limited by its inability to phase match for 1064 nm SHG. The SBO crystal structure was determined. The borate network built from cross-linked chains of $[\text{BO}_4]$ tetrahedra does not fall into one of the structure types having a large SHG effect. Further research is needed to further understand the interesting properties of the SBO crystals.

Acknowledgements

The authors are grateful to Prof. Hu Boqing and Prof. Zhou Tang at the Institute of Physics, Chinese Academy of Science, for assistance in measuring refractive indices, and to Prof. Li Futian at Changchun Institute of Optics, Fine Mechanics and Physics, Chinese Academy of Science, for assistance in the transparency analysis in the vacuum UV region. We also wish to thank

Prof. Zhou Shouhuan of Huabei Institute of Research on Optics and Electricity for the SHG measurement of SBO.

References

- [1] P. Becker, *Adv. Mater.* 10 (1998) 979.
- [2] Wu Yicheng, Tang Honggao, Takatomo Sasaki, et al., *Appl. Phys. Lett.* 62 (1993) 2614.
- [3] Jun-Ming Tu, Douglas A. Keszler, *Mater. Res. Bull.* 30 (1995) 209.
- [4] T.Y. Kwon, J.J. Ju, H.K. Kim, et al., *Mater. Lett.* 27 (1996) 317.
- [5] Chen Chuangtian, Xu Zhuyan, *Appl. Phys. Lett.* 68 (1996) 2930.
- [6] Chuangtian Chen, Yebin Wang, Baichang Wu, et al., *Nature* 373 (1995) 322.
- [7] Yu.S. Oseledchik, A.L. Prosvirnin, A.I. Pisarevskiy, et al., *Opt. Mater.* 4 (1995) 669.
- [8] Liu Hongchao, Guo Changlin, Fan Shiji, Xu Yibin, *J. Inorg. Mater. (Chinese)* 12(1) (1997) 17.
- [9] C.F. Chenot, *J. Am. Ceram. Soc.* 50 (1967) 118.
- [10] A. Perloff, S. Block, *Acta Cryst.* 20 (1966) 274.
- [11] Krogh-Moe, *Acta Chem. Scand.* 18 (1964) 2055.
- [12] Cheng Wendan, Lu Jiayi, *Chinese J. Struct. Chem. (Chinese)* 16(2) (1997) 81.